RESEARCH ARTICLE

Theoretical Morphology and Development of Flight Feather Vane Asymmetry with Experimental Tests in Parrots

JOURNAL OF EXPERIMENTAL ZOOLOGY
PART B
MOLECULAR AND DEVELOPMENTAL EVOLUTION

TERESA J. FEO[1,2]*
AND RICHARD O. PRUM[1,2]

[1]Department of Ecology and Evolutionary Biology, Yale University, New Haven, Connecticut
[2]Peabody Museum of Natural History, Yale University, New Haven, Connecticut

ABSTRACT

Asymmetry in flight feather vane width is a major functional innovation associated with the evolution of flight in the ancestors of birds. However, the developmental and morphological basis of feather shape is not simple, and the developmental processes involved in vane width asymmetry are poorly understood. We present a theoretical model of feather morphology and development that describes the possible ways to modify feather development and produce vane asymmetry. Our model finds that the theoretical morphospace of feather shape is redundant, and that many different combinations of parameters could be responsible for vane asymmetry in a given feather. Next, we empirically measured morphological and developmental model parameters in asymmetric and symmetric feathers from two species of parrots to identify which combinations of parameters create vane asymmetry in real feathers. We found that both longer barbs, and larger barb angles in the relatively wider trailing vane drove asymmetry in tail feathers. Developmentally, longer barbs were the result of an offset of the radial position of the new barb locus, whereas larger barb angles were produced by differential expansion of barbs as the feather unfurls from the tubular feather germ. In contrast, the helical angle of barb ridge development did not contribute to vane asymmetry and could be indicative of a constraint. This research provides the first comprehensive description of both the morphological and developmental modifications responsible for vane asymmetry within real feathers, and identifies key steps that must have occurred during the evolution of vane asymmetry. *J. Exp. Zool. (Mol. Dev. Evol.) 322B:240–255, 2014.* © 2014 Wiley Periodicals, Inc.

J. Exp. Zool. (Mol. Dev. Evol.) 322B:240–255, 2014

How to cite this article: Feo TJ, Prum RO. 2014. Theoretical morphology and development of flight feather vane asymmetry with experimental tests in parrots. J. Exp. Zool. (Mol. Dev. Evol.) 322B:240–255.

A major focus of the field of evolutionary developmental biology has been to identify the role of development in structuring phenotypic diversity (Brakefield, 2006, 2011; Campàs et al., 2010; Hallgrímsson et al., 2012). Feathers display a stunning diversity of form and function both across Aves and within a single individual (Lucas and Stettenheim, '72). Due to their accessibility to experimental manipulation as well as theoretical modeling, feathers are becoming an increasingly popular model for evo-devo studies (Harris et al., 2002, 2005; Yue et al., 2005, 2006; Lin et al., 2006, 2013). Theoretical and experimental research on feather morphogenesis has found that simple changes in feather development can have complex and redundant effects on the final,

Grant sponsor: NSF GRFP; grant sponsor: W. R. Coe Fund, Yale University.
The authors declare no conflict of interest.
*Correspondence to: Teresa J. Feo, Department of Ecology and Evolutionary Biology, Yale University, 21 Sachem St, New Haven, CT 06511. E-mail: teresa.feo@yale.edu
Received 16 December 2013; Revised 20 February 2014; Accepted 15 April 2014
DOI: 10.1002/jez.b.22573
Published online 8 May 2014 in Wiley Online Library (wileyonlinelibrary.com).

mature phenotype (Bleiweiss, '87; Prum and Williamson, 2001; Yue et al., 2006; Badyaev and Landeen, 2007; Alibardi, 2009; Landeen and Badyaev, 2012). Due to this complexity, it is not readily obvious how development is modified in a given feather to produce even simple phenotypes such as vane asymmetry in the flight feathers of wings and tails.

The flight feathers of extant flying birds are generally characterized by an asymmetry in which the leading vane is thinner in width than the relatively wider trailing vane (Lucas and Stettenheim, '72; Speakman and Thomson, '94). Asymmetry in vane width has long been considered an important functional innovation in the evolution of flight (Feduccia and Tordoff, '79; Norberg, '85). The presence of elongated symmetric and asymmetric feathers on the arms, tails, and even legs of non-avian feathered dinosaurs has featured prominently in ongoing debates over when and how flight evolved in the lineage leading to modern birds (Feduccia and Tordoff, '79; Norberg, '85; Xu et al., 2003; Longrich et al., 2012).

Whereas the particular direction of asymmetry in most organismal examples does not appear to serve a specific function (Palmer, 2009), the direction of vane width asymmetry in flight feathers *does* confer specific aerodynamic advantages (Norberg, '85). Both the direction and degree of vane asymmetry contribute to the control of individual feather twisting in airflow during flight (Norberg, '85). A relative reduction in leading vane width effectively shifts the central shaft, or rachis, of the feather closer toward the leading edge. Depending on the degree of asymmetry, the rachis is either positioned at the center of pressure, which minimizes feather twisting in airflow, or ahead of the center of pressure, which causes feathers to twist like venetian blinds; opening on an upstroke and allowing air to pass through the wing, and closing on the downstroke to create a continuous surface (Norberg, '85). This suggests that both the direction and degree of vane width asymmetry in flight feathers are under strong natural selection to maintain a functional aerodynamic phenotype.

Feather vane width asymmetry is a deceptively simple phenotype to characterize; one vane is wider than the other vane. However, vane asymmetry cannot be simply characterized as a developmental modification that grows one vane of the feather more than the other. Any feather phenotype, including vane asymmetry, must instead be understood in terms of the mature branched morphology and tubular development of a feather (Fig. 1a; Prum and Williamson, 2001). Each pennaceous feather vane is comprised of a series branches called barbs that interlock via branching barbules to create a continuous planar surface (Fig. 1b; Lucas and Stettenheim, '72). Non-embryonic feather germs develop as tubes of epidermis that elongate by stem cell division at the base of the follicle (Fig. 1c,d; Lucas and Stettenheim, '72; Yue et al., 2005; Lin et al., 2006). Developing barb ridges differentiate helically such that the tip of a barb forms first on the ventral side of the feather germ and the connection between the base of the barb and the rachis forms last on the dorsal side (Fig. 1d,e; 'Espinasse, '39; Prum, '99; Harris et al., 2002, 2005; Yu et al., 2002; Yue et al., 2006). At the final stage of development, the feather unfurls and expands from its tubular conformation and into its planar mature form (Fig. 1a; Lucas and Stettenheim, '72).

In terms of morphology differences in vane width are achieved by modifying barb length and barb angle (Fig. 1b; Chandler, '14; 'Espinasse, '39; Lucas and Stettenheim, '72; Bleiweiss, '87; Prum and Williamson, 2001). In terms of development several processes have been hypothesiezed to play a role in determing mature vane width by affecting barb length or barb angle. These include the helical angle at which barb ridges develop within the tubular folicle ('Espinasse '39; Bleiweiss, '87; Prum and Williamson, 2001), the expansion of barbs as the feather unfurls ('Espinasse '39; Lucas and Stettenheim, '72; Prum and Williamson, 2001; Maderson et al., 2009), and the radial position of new barb ridge formation relative to the rachis (Strong, '02; Hosker, '36; Lucas and Stettenheim, '72; Prum and Williamson, 2001; Alibardi, 2009). Of these processes, only an offset new barb locus has been demonstrated to occur in real asymmetric feathers (Strong, '02; Hosker, '36; Alibardi, 2009), whereas the other two lack empirical investigation. With the exception of a theoretical model by Prum and Williamson (2001), the effects of these developmental processes on vane width have each been treated separately in past work, and it is unclear how they may interact in concert to produce vane asymmetry in real feathers.

To improve our understanding of the morphological and developmental basis of vane asymmetry in feathers we first formulated a theoretical model that describes vane width in terms of developmental processes that affect mature branched morphology. Next we obtained empirical measurements of all model parameters from asymmetric and symmetric feathers to identify the subset of possible modifications responsible for creating vane asymmetry in flight feathers. By combining our theoretical and empirical results we were able to leverage the advantages of theoretical morphology (McGhee, '99), and identify potential constraints on the development of vane asymmetry.

THEORETICAL MODEL OF VANE WIDTH

We first derive an expression for vane width in terms of barb morphology, and then in terms of feather germ development. All model parameters are diagramed in Figure 2. All angles are measured with respect to the edge of the rachis. The model makes the following four assumptions:

1. The cross-section of the developing feather germ is a circle.
2. Developing feather vanes lie flush around the sides of the cylindrical feather germ with no overlapping barb ridges or vane folding.
3. Individual barb ridges develop at a constant helical angle from barb tip to barb base.
4. Individual barb ridges expand from the feather germ at a constant angle from barb tip to barb base.

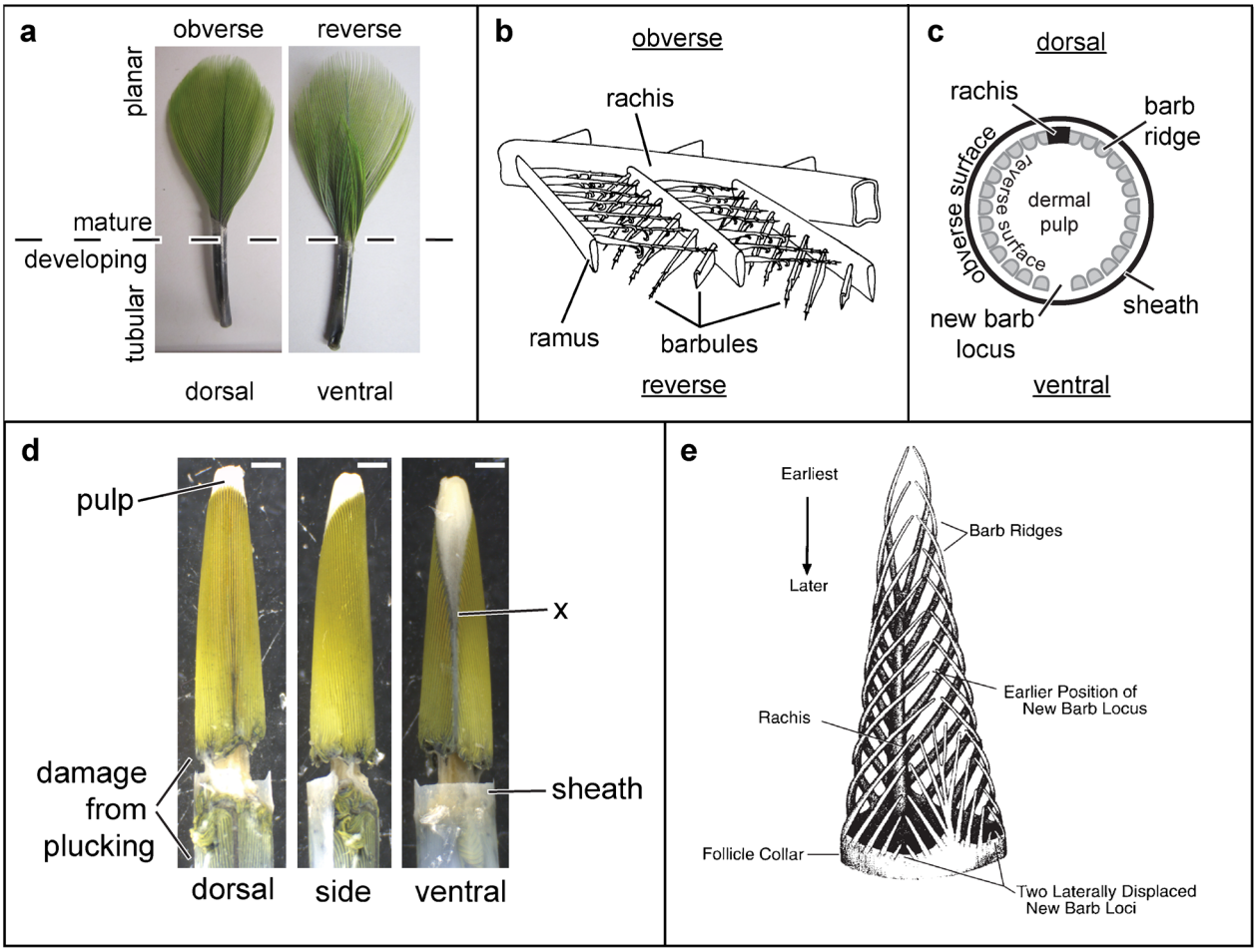

Figure 1. Morphology and development of feathers. a: *Amazona amazonica* upper tail covert plucked mid development. The distal portion of the feather has completed development and has unfurled from the sheath, whereas the proximal portion is still a developing feather germ. Scale bar 5 mm. b: Details of mature feather branches, illustration from Ennos et al. ('95). c: Cross-section of a developing feather germ. d: *A. amazonica* upper tail covert plucked early in development with sheath removed to show the green feather wrapped around the white pulp. X marks the point in development where two new barb loci unite to form a single new barb locus. Note the extensive destruction and folding of the feather surrounding the area where the feather was grasped when plucked. Scale bar 1 mm. e: Diagram of the helical arrangement of barb ridges within the feather germ, illustration from Lucas and Stettenheim ('72).

The last two assumptions imply that mature barbs are straight, and exceptions to these assumptions are discussed below.

Morphology of Vane Width

Consider one vane of a mature, pennaceous, feather composed of a series of barbs attached to the rachis along the length of the feather (Fig. 2a, T_3). The width (W) of the vane at any given position along the length of the feather is the perpendicular distance between the tip of a barb and the rachis. The barb intersects the rachis at a barb angle (A) and has a barb length (L). Vane width can be expressed in terms of barb morphology with the following equation:

$$W = L \sin(A) \tag{1}$$

Vane width (W) will increase with increasing barb length (L) or increasing barb angle (A). Differences between vanes in either of the two parameters would cause vane asymmetry.

Development of Vane Width

Now consider a developing feather germ with radius (r). The rachis is positioned on the dorsal side of the feather germ, and the tip of a barb forms on the ventral side at the new barb locus (Fig. 2a, T_0). In a cross-section of the developing feather germ (Fig. 2b), the rachis

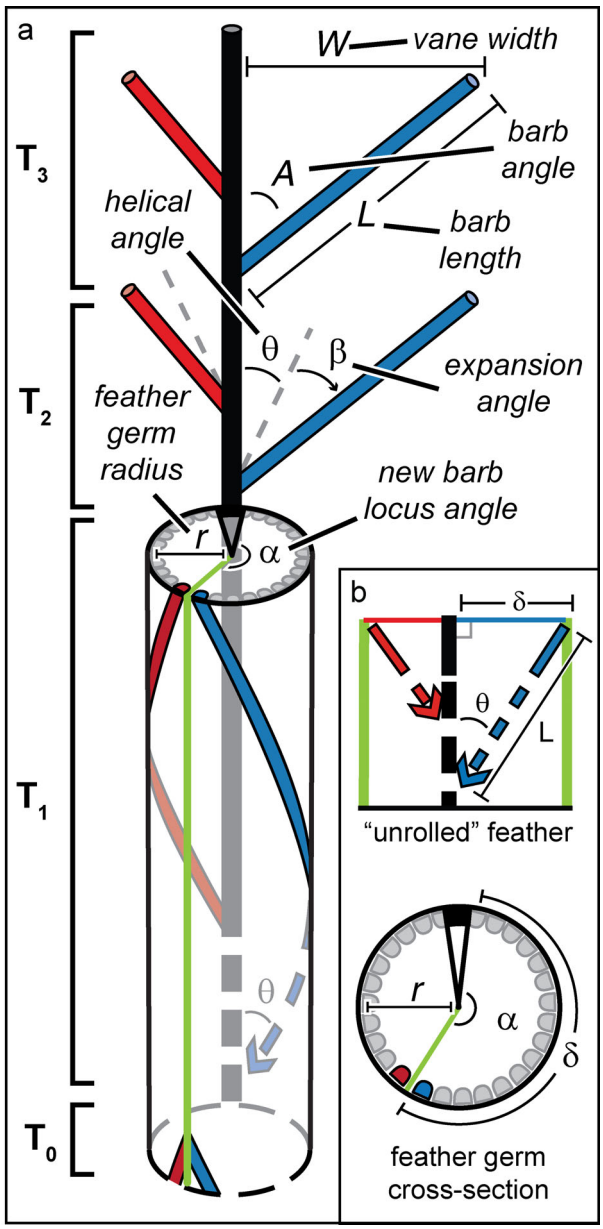

Figure 2. Feather development and the associated vane width model parameters. a: The development of two barbs from start to finish. T_0: new barb tips (in red or blue) form at the new barb locus (green line) on the ventral side of the feather germ. T_1: barbs grow helically around the feather germ at an angle θ until they meet the rachis (heavy black line) on the dorsal side. T_2: at the completion of development the sheath breaks away allowing the feather to unfurl and barbs to expand by and additional angle β. T_3: barbules interlock (not shown) and the feather reaches its mature, planar form. b: Details of barb length (*L*) development. The distance (δ) between a new barb tip and the rachis is represented as the arc between the rachis and the new barb locus.

and new barb locus specify an arc with a subtending angle (α), hereafter referred to as the new barb locus angle. The linear distance (δ) between the new barb locus and the rachis can be represented as the arc length between the new barb locus and the rachis:

$$\delta = \alpha r \tag{2}$$

As cell proliferation and differentiation progress at the base of the developing feather germ, the barb ridge elongates helically around the developing feather germ at a helical angle (θ) until it meets with the rachis on the dorsal side of the feather germ (Fig. 2a, T_1). The development of mature barb length (*L*) can be expressed as:

$$L = \frac{\alpha r}{\sin(\theta)} \tag{3}$$

The feather germ is pushed out of the follicle as new cells are added to the proximal end of the feather germ. When the protective sheath breaks away from the mature, distal end of the feather germ, the feather unfurls (Fig. 1a). Barbs may undergo an additional expansion by angle (β) as the feather unfurls into a flat plane (Fig. 2a, T_2). The barb angle (*A*) of a mature feather can be expressed in terms of development as:

$$A = \theta + \beta \tag{4}$$

Substituting Equations (3) and (4) into Equation (1) gives feather vane width in terms of developmental processes:

$$W = \frac{\alpha r}{\sin(\theta)} \sin(\theta + \beta) \tag{5}$$

Vane width (*W*) will increase with increasing follicle radius (*r*), expansion angle (β) or new barb locus angle (α). Conversely, vane width will decrease with increasing helical angle (θ), so long as expansion angle (β) is greater than zero. This is because a barb that develops with a larger helical angle will reach the rachis "sooner" resulting in a shorter barb. Expansion angle would then have a relatively smaller effect on the final width of the feather.

Differences between vanes in helical angle (θ), expansion angle (β), or new barb locus angle (α) would cause vane width asymmetry. The model demonstrates that the developmental and morphological basis of vane width is redundant and many different possible combinations of parameters could be used to achieve vane asymmetry in a given feather.

Barb Curvature

Our models make the simplifying assumptions that barb ridges are straight during development and at maturity. However, it is common for feathers to curve either in toward or away from the feather tip (e.g., Fig. 1a; Lucas and Stettenheim, '72). Curving barbs implies that either helical angle or expansion angle varied along the length of a barb. To accommodate this process in our models, we would need to replace the constants θ or β in

Equation (5) with a function describing how the angle changed along the length of a barb. Investigating the details of how barb curvature develops is beyond the scope of this paper, but we can nevertheless describe the overall affects of barb curvature on mature vane width.

Assuming a straight barb, the predicted vane width (W_p) can be calculated by using measured values of barb angle (A_m) and barb length (L_m). The difference between the measured vane width (W_m) from the feather, and the predicted vane width (W_p), would represent the affect of barb curvature.

$$C = W_m - W_p; \text{where } W_p = L_m \sin(A_m) \quad (6)$$

When barbs are nearly straight the value for C will be close to zero. When barbs curve convexly toward the feather tip C will be negative, representing a reduction in the possible vane width as a result of barb curvature. As barbs curve concavely away from the feather tip, C will first become positive as curvature increases vane width, and then become negative once barbs begin to curve back on themselves reducing vane width.

EXPERIMENTAL METHODS

Our models predict that several characters could contribute to vane width asymmetry at both the morphological and developmental level. In order to determine which of many possible combinations of characters is responsible for vane width asymmetry in real feathers we obtained empirical measures of all model parameters. We collected symmetrical upper tail coverts and asymmetrical outer rectrices (Fig. 3a,b) from Orange-winged Amazon Parrots (Psittacidae: *Amazona amazonica*) and Grey Cockatiel (*Nymphicus hollandicus*). Feather vanes were measured at a distal position close to the feather tip, and a proximal position close to the midpoint to capture how characters changed both between vanes, and along the length of feathers (Fig. 3c). This resulted in a set of measured characters at four locations for each feather: distal trailing vane, distal leading vane, proximal trailing vane, and proximal leading vane.

It was not possible to measure all model parameters from a single rectrix or covert, and we instead collected a series of homologous mature feathers and regenerating feather germs from each bird (Fig. 3c). Each parameter at a given location was measured once from an appropriate feather in the homologous series, and the measures were pooled together to obtain a complete set of measurements for each bird and feather type. We compared measures of barb angle, barb length, and vane width within series of homologous, asymmetric feathers collected from 10 *A. amazonica* and found that parameters at a given location were highly correlated within each individual (Pearsons corr > 0.8, $P < 0.01$).

Feather Plucking

Feathers were collected from adult, captive birds belonging to long term breeding colonies maintained by the Meyer Hall and Hopkins Avian Facilities in the Department of Animal Sciences at the University of California, Davis. The sample of *A. amazonica* were a mix a males, females, and individuals of unknown sex, whereas all *N. hollandicus* were females. Birds were kept in their colony under normal conditions throughout the course of the experiments.

We plucked the pair of outer rectrices (R6) and a pair of central coverts from each bird. Plucking feathers generally induces the

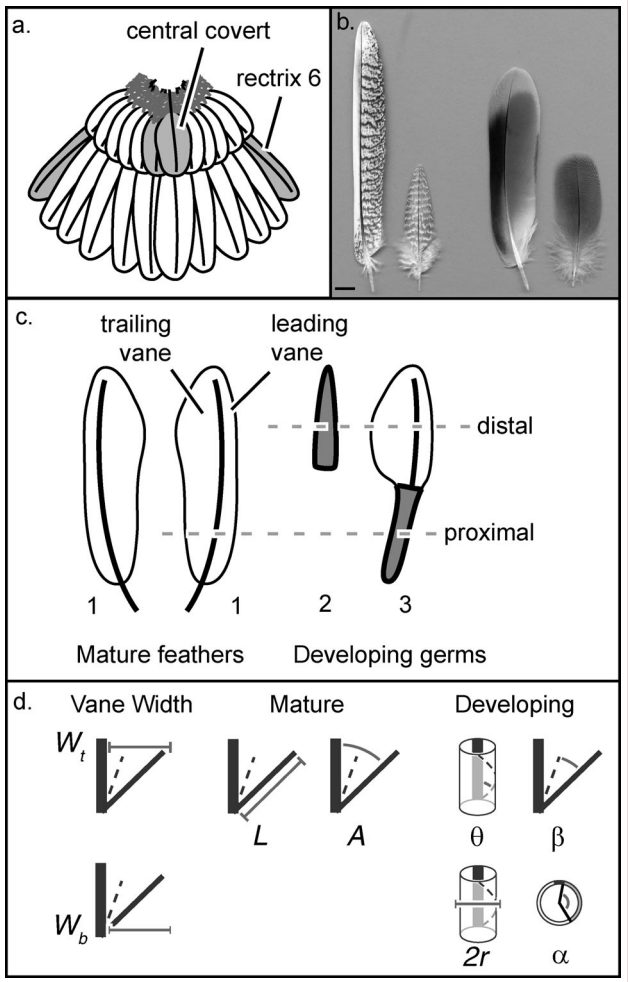

Figure 3. Plucking experiments and character measurements. a: Location within the tail of symmetrical, upper trail coverts and asymmetrical, rectrix 6. b: Photo of rectrices and coverts from *N. hollandicus* (left) and *A. amazonica* (right). Scale bar 10 mm. c: Diagram of homologous series of mature feathers and developing feather germs collected from each bird and feather type. Numbers indicate relative timing when feather or germ was plucked. Dotted line indicates relative position of distal and proximal measurements. d: Diagram of parameter measurements detailing which character measures are associated with vane width measured at the barb tip and barb base.

growth of replacement feathers. Once they were visible above the skin, replacement *N hollandicus* feather germs grew an average of 3–4 mm/day. Within 2–3 weeks, the tips of four replacement feather germs were projecting above the skin but still covered with the sheath. A rectrix and covert feather germ was plucked from each bird at this early stage of feather regeneration to provide a sample of the distal feather tip in development (Fig. 3c). After an additional 1–3 weeks, the distal portion of the remaining two feather germs had completed development and unfurled from the sheath, while a more proximal portion of the feather germ was covered with sheath (see Fig. 1a for example). The remaining rectrix and covert from each bird were plucked at this later stage to sample the development of a proximal part of the feather (Fig. 3c).

Mature feathers were plucked by hand and developing feather germs were plucked by grasping them firmly with hemostats just above the level of the skin. We found that the use of hemostats greatly reduced the chance of the feather germ breaking into pieces. If a portion of a broken feather germ remains in the follicle it will cause bleeding until it is removed. Unfortunately, the barb ridges were destroyed where the hemostats grasped the feather germ, but this conveniently marked the position of the skin for future reference (Fig. 1d).

We found that 80–100% of the rectrices from both species, as well as *N. hollandicus* coverts grew back within the time frame of the experiment. Unfortunately, only about half of the *A. amazonica* coverts grew back during the course of the experiment. We suspect that the delayed covert feather regeneration was due to the fact that the birds were approaching their breeding season. We have found that actively laying, female chicken and quail grow back $<50\%$ of their plucked contour feathers, whereas males grow back most of their contour feathers (T.J. Feo, pers. obs.). As a result we were unable to obtain a complete sample of symmetrical feather development in *A. amazonica*, and are only able to present results for the development of the distal feather tip.

Feather Preparation

Mature feathers were cleaned with a damp paper towel and "preened" by hand to repair any overlapping or separated barbs. For developing feather germs, we first cut off and saved any distal portion of the feather that had already unfurled from the sheath. Next we carefully removed the sheath to expose the obverse surface of the feather still wrapped around the dermal pulp or pulp caps (Fig. 1c,d). Even with the sheath removed, the developing feather will not unfurl from its tubular arrangement as long as the barbs are not severely disturbed and the feather germ does not dry out. Mature feathers were stored dry in plastic bags and feather germs were stored in vials of 70% ethanol.

The portion of the feather in sheath but above the level of the skin was rigid, and the structural blues and greens in the *A. amazonica* feathers were present, indicating that the feather cells must already have been keratinized and fully developed (Prum et al., 2009). Below the level of the skin the feather was clearly still in a process of developing; the feather was soft, portions that would be blue or green at maturity were black, and the sheath could not be easily separated from the feather without damaging the barb ridges. All developmental measurements were taken from the portion of the feather germ in sheath and above the level of the skin.

Character Measurements

We scanned the reverse surface of mature feathers with an Epson Perfection 4180 Photo scanner at 2400 dpi and saved scans as black and white .tif images. We imaged the dorsal surface of developing feather germs where the barbs meet the rachis with a camera attached to a Leica dissecting microscope. We used imagej (http://rsbweb.nih.gov/ij/) with the objectj plugin (http://simon.bio.uva.nl/objectj/) to take measurements from the images.

Only a small portion of the feather was in sheath at any given time, and as a result any sampled tubular feather germ contained the bases of barbs but not their tips and vice versa. All developmental characters were measured at the midpoint of the tubular portion of the feather germ above the skin. Morphological characters were measured from a barb whose base intersected the rachis at an equivalent position from the tip. The developmental characters either corresponded to a barb whose base intersected the rachis at the measurement position, or to a barb whose tip first formed at that position (Fig. 3d). Measures of new barb locus angle (α), feather germ diameter ($2r$) therefore correspond to a vane width measured at the mature barb base (W_b) and all other characters correspond to vane width measured at the mature barb tip (W_t).

Mature barb angle (A), barb length (L), and vane widths (W_t, W_b) were measured from scans of mature feathers. Curvature error (C) was calculated as the difference between measured vane width (W_t) and predicted vane width (W_t) as described in Equation (6). Helical angle (θ) and feather germ diameter ($2r$) were measured from images of developing feather germs, and barb expansion angle (β) was calculated as the difference between barb angle (A) and helical angle (θ) as described in Equation (4).

The angular position of the new barb locus (α) for each vane was measured from feather germs as the rotation angle between the edge of the rachis and the edge of a vane. An insect pin was inserted through the center of developing feather germs and then horizontally mounted to a Siskiyou RSX 1.0 rotation stage placed under a dissecting microscope. The new barb locus angle was recorded as the number of degrees required to rotate the feather germ between a centered view of the rachis edge and the vane edge. This method for measuring the relative distance between the rachis and the edge of a vane within a developing feather follicle worked well. As a test we compared rachis width measured from images with rachis width calculated from rotation angle and found the two were highly correlated with an average error less than 0.1 mm (Pearsons corr >0.95, $P<0.01$).

Statistical Analysis

For feathers with complete data sets, we conducted two-way repeated-measures ANOVA on each parameter with measurement position along the length of feathers (distal, proximal) and feather vane (leading, trailing) as factors. Significant results were followed with paired Bonferroni *post hoc* tests to determine how parameters varied within feathers. Paired *t*-tests were used to compare the developmental characters measured from the distal vanes of *A. amazonica* coverts, and for feather germ diameter ($2r$) between distal and proximal positions for all feather types. Parameter measures are presented in Table 1 as mean ± SD. Differences between vanes were calculated as trailing vane minus leading vane for each feather and then averaged. Differences between positions were calculated as proximal minus distal for each feather and then averaged.

RESULTS

There was little qualitative difference in how characters varied within feathers between *N. hollandicus* and *A. amazonica* unless otherwise noted. Character measures are summarized in Table 1, the results of ANOVA tests are summarized in Table 2, difference between leading and trailing vanes are summarized in Table 3, and differences between distal and proximal positions along the length of vanes are summarized in Table 4.

Vane Width Morphology

Vane width. Covert feathers were symmetric in vane width and vane width increased proximally along the length of coverts (Fig. 4). Rectrix vane width asymmetry was low at the distal tip and increased proximally due to large increases in trailing vane width and little to no change in leading vane width.

Table 1. Empirical measures of model parameters in symmetric coverts and asymmetric rectrix feathers.

	Coverts				Rectrices			
	N. hollandicus ($n = 13$)		*A. amazonica* ($n = 15$)		*N. hollandicus* ($n = 14$)		*A. amazonica* ($n = 15$)	
	Leading	Trailing	Leading	Trailing	Leading	Trailing	Leading	Trailing
Vane width								
At barb tip (mm)—W_t								
Distal	1.6 ± 0.3	1.4 ± 0.3	2.4 ± 0.7	2.5 ± 0.5	1.9 ± 0.4	3.1 ± 0.7	3.1 ± 0.9	4.3 ± 1.4
Proximal	5.0 ± 0.6	5.0 ± 0.7	11.3 ± 0.9	11.1 ± 1.3	3.7 ± 0.5	12.5 ± 0.9	6.9 ± 1.5	15.3 ± 2.6
At barb base (mm)—W_b								
Distal	4.0 ± 0.7	3.8 ± 0.5	10.6 ± 0.8	10.5 ± 1.1	2.5 ± 0.5	8.5 ± 1.1	7.6 ± 1.1	15.6 ± 1.6
Proximal	7.0 ± 0.6	6.5 ± 0.7	11.4 ± 1.2	11.4 ± 1.1	3.6 ± 0.5	12.4 ± 0.9	5.8 ± 1.4	15.8 ± 1.7
Morphological characters								
Barb length (mm)—L								
Distal	7.7 ± 1.0	7.9 ± 0.9	13.9 ± 1.6	13.9 ± 1.6	6.8 ± 1.0	11.9 ± 1.9	13.6 ± 1.2	14.6 ± 1.0
Proximal	14.1 ± 0.8	14.3 ± 1.0	23.8 ± 2.1	23.9 ± 1.9	14.2 ± 1.5	27.0 ± 1.8	15.5 ± 2.8	25.9 ± 2.3
Barb angle (°)—A								
Distal	18.8 ± 2.0	17.6 ± 2.4	16.2 ± 2.5	16.6 ± 2.0	20.9 ± 1.8	22.4 ± 2.3	16.9 ± 2.7	18.8 ± 3.5
Proximal	30.4 ± 3.6	28.9 ± 4.1	43.5 ± 3.7	43.0 ±2.7	17.4 ± 2.2	31.6 ± 1.9	23.9 ± 3.5	35.3 ± 4.8
Curvature error (mm)—C								
Distal	−0.9 ± 0.3	−0.9 ± 0.3	−1.5 ± 0.7	−1.5 ± 0.6	−0.5 ± 0.2	−1.4 ± 0.6	−0.8 ± 0.6	−0.4 ± 1.0
Proximal	−2.0 ± 0.5	−1.9 ± 0.7	−5.0 ± 1.8	−5.1 ± 1.8	−0.4 ± 0.2	−1.6 ± 0.7	0.7 ± 0.5	0.5 ± 1.8
Developmental characters								
Helical angle (°)—θ								
Distal	5.9 ± 0.6	5.4 ± 0.5	4.9 ± 0.9	5.1 ± 0.8	9.7 ± 0.9	8.3 ± 1.0	6.4 ± 1.1	7.1 ± 1.1
Proximal	7.1 ± 0.9	7.3 ± 0.9	–	–	9.3 ± 1.3	12.9 ± 1.0	10.8 ± 1.7	12.1 ± 2.0
Expansion angle (°)—β								
Distal	12.9 ± 1.8	12.2 ± 2.3	11.3 ± 2.5	11.5 ± 1.8	11.3 ± 1.9	14.1 ± 2.1	10.5 ± 2.1	11.7 ± 3.0
Proximal	23.3 ± 3.3	21.6 ± 3.7	–	–	8.0 ± 2.2	18.7 ± 1.5	13.2 ± 3.0	23.2 ± 3.4
New barb locus (°)—α								
Distal	171 ± 10	175 ± 11	176 ± 5	184 ± 5	101 ± 16	211 ± 10	137 ± 14	213 ± 9
Proximal	167 ± 5	169 ± 5	–	–	129 ± 7	198 ± 7	130 ± 10	202 ± 10
Germ diameter (mm)—$2r$								
Distal	1.0 ± 0.1		2.2 ± 0.1		1.6 ± 0.1		2.7 ± 0.2	
Proximal	1.4 ± 0.1		–		2.3 ± 0.1		2.9 ± 0.2	

Table 2. Summary statistics of two-way repeated measure ANOVA's.

	Coverts		Rectrices	
	N. hollandicus F (1,12)	*A. amazonica* F (1,14)	*N. hollandicus* F (1,13)	*A. amazonica* F (1,14)
Vane width				
At barb tip—W_t				
Position	416.9*	1263.5*	792.5*	377.7*
Vane	0.7	0.1	1199.7*	119.2*
Interaction	0.1	1.6	1067.6*	72.3*
At barb base—W_b				
Position	499.1*	15.7*	165.8*	12.2*
Vane	10.0*	0.1	2055.7*	293.6*
Interaction	2.1	0.1	69.5*	63.4*
Morphological characters				
Barb length—L				
Position	744.8*	306.4*	316.3*	194.6*
Vane	1.7	0.2	964.7*	145.2*
Interaction	0.002	0.1	527.8*	163.0*
Barb angle—A				
Position	149.3*	1071.0*	67.8*	176.1*
Vane	4.4	0.01	288.4*	116.0*
Interaction	0.004	0.7	282.1*	89.8*
Curvature—C				
Position	59.4*	69.8*	0.02	12.0*
Vane	0.2	0.2	120.3*	0.3
Interaction	1	0.3	1.9	1.4
Developmental characters				
Expansion angle—β				
Position	154.6*	–	2.3	75.2*
Vane	2.8	–	178.3*	77.6*
Interaction	0.5	–	72.9*	73.5*
Helical angle—θ				
Position	28.9*	–	61.4*	184.4*
Vane	0.9	–	37.9*	22.2*
Interaction	9.8*	–	107.8*	6.9*
New barb locus—α				
Position	6.96*	–	10.4*	57.2*
Vane	1.3	–	608.9*	234.0*
Interaction	0.1	–	73.3*	0.5

*$P < 0.02$, otherwise $P > 0.05$.

Barb length and barb angle. Neither barb length nor barb angle differed significantly between the vanes of symmetric coverts, and both characters increased proximally with increasing vane width (Fig. 5a,b,e,f,i,j). There was little to no difference in barb length and barb angle between rectrix vanes at the distal tip where vane width asymmetry was low (Fig. 5c,d,g,h,k,l). As rectrix vane width asymmetry increased proximally, barb length and barb angle became relatively large in the wider trailing vane compared with little or no change in the thinner leading vane. Barb length and barb angle showed similar patterns of change in both coverts and rectrices; both morphological characters increased with increasing vane width within a feather.

Barb curvature. The barbs in all feathers we examined curved in toward the rachis at their tips. As a result, the measured vane width was generally smaller than the predicted width assuming straight

Table 3. Measured character differences between trailing (Tr) and leading (Ld) vane.

	Coverts				Rectrices			
	N. hollandicus ($n = 13$)		*A. amazonica* ($n = 15$)		*N. hollandicus* ($n = 14$)		*A. amazonica* ($n = 15$)	
	Tr–Ld	*P*	Tr–Ld	*P*	Tr–Ld	*P*	Tr–Ld	*P*
Vane width								
At barb tip (mm)–W_t								
Distal	-0.1 ± 0.2	ns	0.1 ± 0.6	ns	1.2 ± 0.4	<.01	1.2 ± 0.9	<.01
Proximal	-0.1 ± 0.7	ns	-0.2 ± 1.1	ns	8.7 ± 0.9	<.01	8.4 ± 3.2	<.01
At barb base (mm)–W_b								
distal	-0.2 ± 0.4	.05	-0.1 ± 1.1	ns	6.1 ± 0.8	<.01	8.0 ± 1.8	<.01
proximal	-0.6 ± 0.7	ns	-0.0 ± 1.1	ns	8.8 ± 0.9	<.01	10.0 ± 2.3	<.01
Morphological characters								
Barb length (mm)–*L*								
Distal	0.2 ± 0.2	ns	0.0 ± 0.5	ns	5.1 ± 1.3	<.01	1.0 ± 0.9	<.01
Proximal	0.1 ± 0.8	ns	0.1 ± 1.0	ns	12.8 ± 1.2	<.01	10.4 ± 3.2	<.01
Barb angle (°)–*A*								
Distal	-1.2 ± 1.5	ns	0.4 ± 3.0	ns	1.5 ± 1.5	<.01	1.9 ± 2.3	0.04
Proximal	-1.2 ± 3.5	ns	-0.5 ± 2.8	ns	14.3 ± 2.8	<.01	11.4 ± 3.7	<.01
Curvature (mm)–*C*								
Distal	-0.0 ± 0.3	ns	0.0 ± 0.5	ns	-0.9 ± 0.5	<.01	0.5 ± 0.8	ns
Proximal	0.1 ± 0.7	ns	-0.2 ± 1.3	ns	-1.2 ± 0.6	<.01	-0.2 ± 1.8	ns
Developmental characters								
Helical angle (°)–θ								
Distal	-0.4 ± 0.8	ns	0.2 ± 0.6	ns	-1.4 ± 1.3	<.01	0.7 ± 0.6	<.01
Proximal	0.1 ± 0.5	ns	–	–	3.6 ± 0.9	<.01	1.3 ± 1.2	<.01
Expansion angle (°)–β								
Distal	-0.7 ± 1.6	ns	0.2 ± 2.8	ns	2.9 ± 1.9	<.01	1.2 ± 2.2	ns
Proximal	-1.4 ± 3.6	ns	–	–	10.7 ± 3.1	<.01	10.1 ± 3.9	<.01
New barb locus (°)–α								
Distal	4 ± 16	ns	8 ± 10	<.01	109 ± 18	<.01	76 ± 22	<.01
Proximal	2 ± 9	ns	–	–	69 ± 13	<.01	72 ± 19	<.01

P-values for paired post-hoc comparisons or paired *t*-tests. ns represents $P > 0.1$.

barbs (Fig. 5m–p). The effects of barb curvature on vane width were larger in coverts than rectrices. The percent difference between predicted and measured vane width was as a high as 40% in the *N. hollandicus* coverts. This suggests that barb curvature can have substantial impact on final vane width.

Vane Width Development

Expansion angle. Expansion angle did not significantly differ between the vanes of symmetric coverts, and showed large (~10°) increases proximally with increasing vane width in *N. hollandicus* coverts (Fig. 6a,b,e,f). There was little to no significant difference in expansion angle between rectrix vanes at the distal tip where vane width asymmetry was low (Fig. 6c,d,g,h). As rectrix vane width asymmetry increased proximally, differences in expansion angle between vanes became large (~10°). This was due to relatively large increases in expansion angle in the wider trailing vane compared to little or no change in the thinner leading vane. In both coverts and rectrices expansion angle showed large increases with increasing vane width within a feather.

Helical angle. Helical angle did not significantly differ between the vanes of symmetric coverts (Fig. 6a,b,i,j), and showed only a small (~1–2°) significant increase proximally with increasing vane width in *N. hollandicus* coverts (Fig. 6a,i). At both the tips of rectrices where vane width asymmetry was small, and at more proximal positions where vane width asymmetry was large, there were only small (<4°) significant differences in helical angle between rectrix vanes (Fig. 6c,d,k,l). Helical angle also showed only small (<5°) increases proximally with increasing rectrix

Table 4. Measured character differences between proximal (Pr) and distal (Dt) positions within vanes.

	Coverts				Rectrices			
	N. hollandicus ($n = 13$)		*A. amazonica* ($n = 15$)		*N. hollandicus* ($n = 14$)		*A. amazonica* ($n = 15$)	
	Pr–Dt	*P*	Pr–Dt	*P*	Pr–Dt	*P*	Pr–Dt	*P*
Vane width								
At barb tip (mm)—W_t								
Leading	3.5 ± 0.6	<.01	8.9 ± 0.8	<.01	1.9 ± 0.5	<.01	3.8 ± 1.9	<.01
Trailing	3.5 ± 0.9	<.01	8.6 ± 1.3	<.01	9.3 ± 1.1	<.01	11.0 ± 2.5	<.01
At barb base (mm)—W_b								
Leading	3.0 ± 0.6	<.01	0.8 ± 1.1	ns	1.2 ± 0.4	<.01	−1.8 ± 0.9	<.01
Trailing	2.7 ± 0.6	<.01	0.9 ± 1.0	.02	3.9 ± 1.3	<.01	0.2 ± 1.1	ns
Morphological characters								
Barb length (mm)—*L*								
Leading	6.4 ± 1.0	<.01	9.9 ± 2.5	<.01	7.3 ± 2.0	<.01	2.0 ± 2.5	.06
Trailing	6.4 ± 0.9	<.01	9.9 ± 2.1	<.01	15.0 ± 2.8	<.01	11.3 ± 2.1	<.01
Barb angle (°)—*A*								
Leading	11.3 ± 3.1	<.01	27.3 ± 4.6	<.01	−3.7 ± 2.0	<.01	7.0 ± 3.5	<.01
Trailing	11.3 ± 4.3	<.01	26.4 ± 2.5	<.01	9.2 ± 2.0	<.01	16.5 ± 4.3	<.01
Curvature (mm)—*C*								
Leading	−1.1 ± 0.4	<.01	−3.5 ± 1.8	<.01	0.1 ± 0.2	ns	1.5 ± 0.9	<.01
Trailing	−0.9 ± 0.7	<.01	−3.7 ± 1.8	<.01	−0.2 ± 0.9	ns	0.8 ± 2.2	ns
Developmental characters								
Helical angle (°)—θ								
Leading	1.2 ± 1.0	<.01	–	–	−0.3 ± 1.6	<.01	4.3 ± 1.2	<.01
Trailing	1.8 ± 1.1	<.01	–	–	4.6 ± 1.1	<.01	4.9 ± 1.5	<.01
Expansion angle (°)—β								
Leading	10.1 ± 2.8	<.01	–	–	−3.4 ± 2.3	<.01	2.7 ± 3.6	.07
Trailing	9.5 ± 3.7	<.01	–	–	4.6 ± 2.3	<.01	11.5 ± 3.9	<.01
New barb locus (°)—α								
Leading	−4 ± 10	ns	–	–	27 ± 15	<.01	−7 ± 11	ns
Trailing	−6 ± 12	ns	–	–	−13 ± 9	<.01	−11 ± 9	<.01
Germ diameter (mm)—2*r*	0.3 ± 0.1	<.01	–	–	0.7 ± 0.1	<.01	0.2 ± 0.1	<.01

P-values are from paired post-hocs comparisons or paired *t*-tests. ns represents $P > 0.1$.

vane width. In both coverts and rectrices helical angle varied only slightly within a feather despite large changes in vane width.

New barb locus angle. There was little to no significant difference in new barb locus angle between the vanes of symmetric coverts, and no significant increase in new barb locus angle along the length of *N. hollandicus* coverts despite increases in vane width (Fig. 7a,b,e,f). However, there were large differences in new barb locus angle between rectrix vanes where vane width asymmetry was also relatively large (Fig. 7c,d,g,h). New barb locus angle generally showed little to no change along the length of rectrix vanes with little to no change in vane width. The exception was the leading vane of *N. hollandicus*, in which new barb locus angle increased by an average of 27° along the length of the vane (Fig. 7g). In general, there were large differences between vanes in new barb locus angle with large vane width asymmetry and little change in new barb locus angle along the length of a feather even despite increases in vane width.

Feather germ diameter. Feather germ diameter increased proximally with increasing vane width for all feather types (Fig. 7a–d,i–l).

Barb Angle and Barb Length Development

Mature barb angle is the sum of expansion angle and helical angle (Equation 4). We found that expansion angle always provided a larger contribution to the final mature barb angle than helical

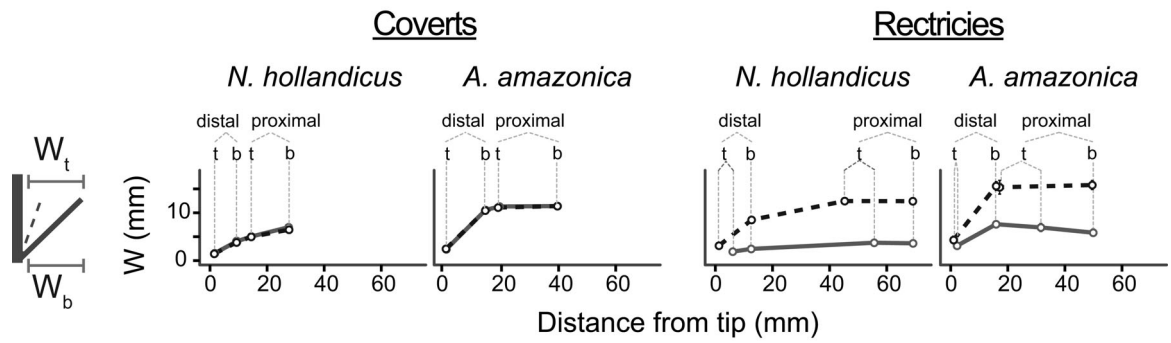

Figure 4. Average vane width of trailing vane (dotted black) and leading vane (solid gray) along length of feathers. At distal and proximal positions along the length of feathers, vane width was measured at the tip (t) and base (b) of a selected barb. Covert vane width was symmetric and became wider proximally along the length of the feathers. Asymmetry in rectrices was low at the feather tip and increased proximally due to relatively large increases in trailing vane width. Error bars are 95% confidence intervals.

angle (paired t-test, all $P < .05$), with the exception of a similar helical and expansion angle in the leading vane of *N. hollandicus* rectrices ($P = .1$). Large changes in barb angle within a feather also appeared to be driven by changes in expansion angle rather than in helical angle (Figs. 5i–l and 6e–l). Large differences in mature barb angle ($>10°$) within a feather were accompanied by large differences in expansion angle ($>10°$) and only relatively small changes in helical angle (1–5°).

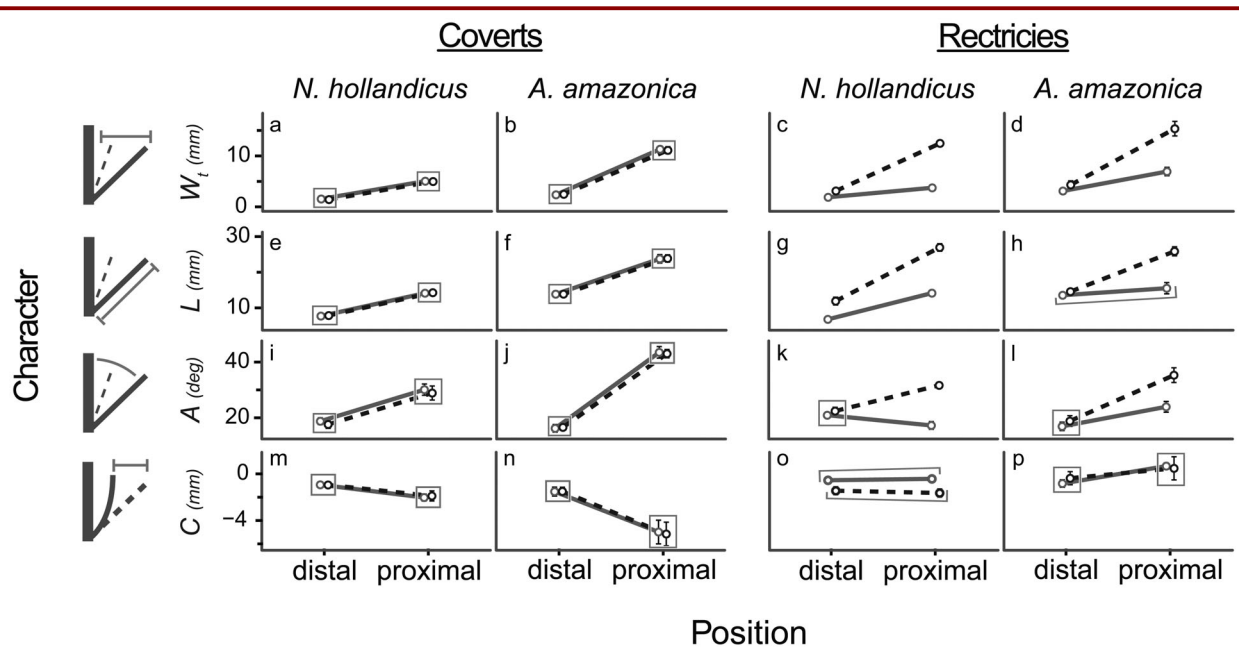

Figure 5. Comparison of average changes in mature vane width and barb morphological characters within trailing vanes (dotted black) and leading vanes (solid gray) of symmetric coverts and asymmetric rectrices. a–d: vane width (W_t), e–h: barb length (L), i–l: barb angle (A), and m–p: barb curvature (C). Barb length and barb angle did not differ between vanes of symmetric coverts, and both increased proximally with increasing vane width. Differences in both morphological characters between rectrix vanes increased proximally with increasing vane width asymmetry due to relatively large increases in the trailing vane. The effects of curvature vary within feathers and in coverts curvature reduces the possible vane width by upwards of 40%. Gray boxes surround character measures that are not significantly different ($P > 0.05$), error bars represent 95% confidence intervals.

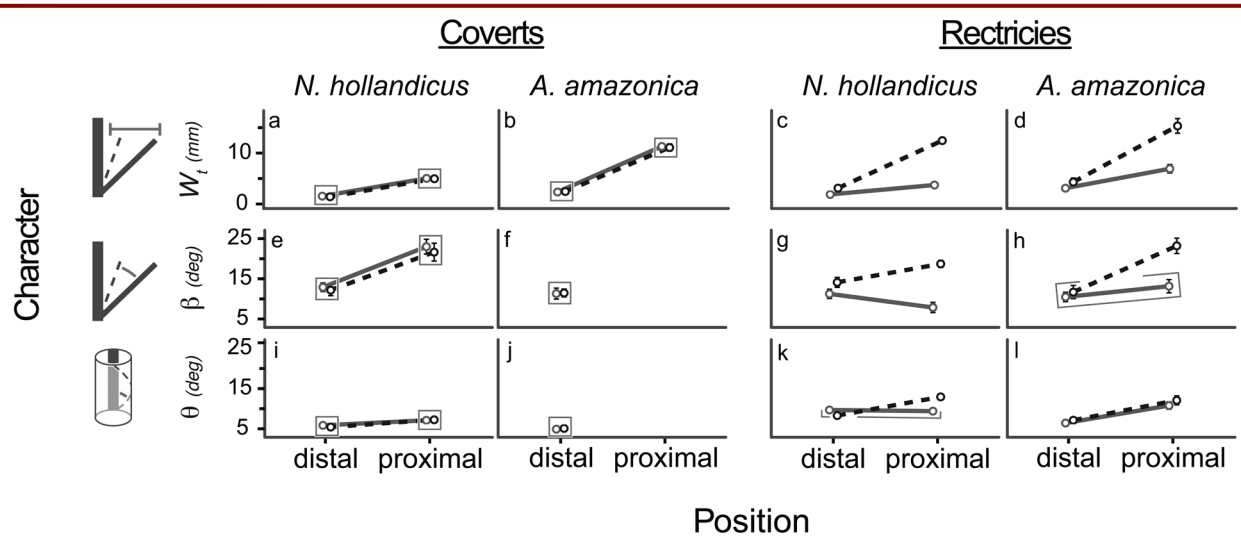

Figure 6. Comparison of average changes in mature vane width and developmental characters within trailing vanes (dotted black) and leading vanes (solid gray) of symmetric coverts and asymmetric rectrices. a–d: vane width (W_t), e–h: expansion angle (β), and i–l: helical growth angle (θ). Expansion angle did not differ between the vanes of symmetric coverts, and increased proximally with increasing vane width. Differences in expansion angle between rectrix vanes were low at the tips, and increased proximally with increasing vane width asymmetry due to relatively large increases in the trailing vane. In comparison, there was relatively little change in helical angle within either coverts or rectrices despite large changes in vane width. Gray boxes surround character measures that are not significantly different ($P > 0.05$), error bars represent 95% confidence intervals.

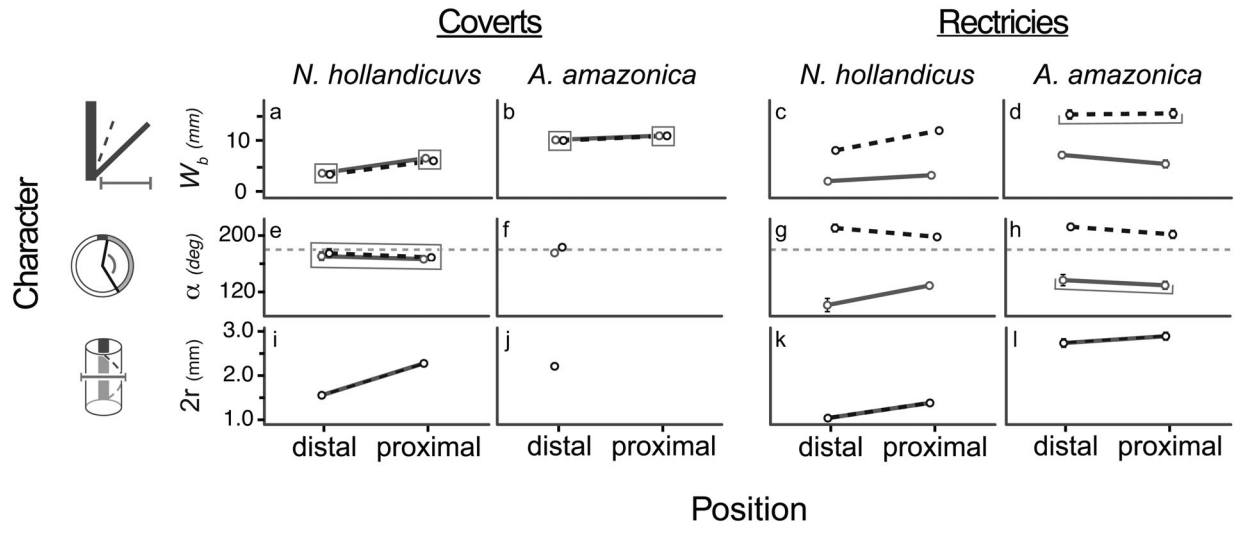

Figure 7. Comparison of average changes in mature vane width and developmental characters within trailing vanes (dotted black) and leading vanes (solid gray) of symmetric coverts and asymmetric rectrices. a–d: vane width (W_b), e–h: new barb locus angle (α), and i–l: feather germ diameter ($2r$). New barb locus angle does not differ between vanes of symmetric coverts and does not change along the length of feathers despite increasing vane width. Differences in new barb locus angle between rectrix vanes were large where rectrix asymmetry was high. Feather germ diameter increases with increasing vane width in both coverts and rectrices. Gray boxes surround character measures that are not significantly different ($P > 0.05$), error bars represent 95% confidence intervals.

Differences in barb length between vanes could be driven by differences in helical angle or new barb locus angle, and differences along the length of a feather could be driven by these two characters as well as feather germ radius (Equation 3). Increases in barb length within a feather (Fig. 5e–h), were generally associated with increases in helical angle (Fig. 6i–l). However according to our model (Equation 3), increasing helical angle would have a *negative* affect on barb length. This suggests that helical angle did not positively contribute to the observed changes in barb length within a feather.

New barb locus angle differed between vanes with asymmetric barb length but showed little to no change when barb length increased along the length of a feather (Fig. 7e–h). This suggests that offsetting the new barb locus (Fig. 7e–h) was the main cause of barb length differences between vanes, whereas increasing feather germ radius (Fig. 7i–l) mainly drove barb length increases along the length of vanes. In the case of the leading vane of *N. hollandicus* rectrices, both an increasing feather germ diameter and a large increase in new barb locus angle contributed to increases in barb length (Fig. 7g,k).

Arrangement of the Developing Feather

The very tips of developing feathers did not completely span the entire circumference of the feather germ, resulting in a gap between vane edges (Fig. 1d). This gap generally closed within a few millimeters below the feather tip (Fig. 1d), and was not present at the distal measure of new barb locus angle for most feathers (Fig. 8a,c,f). However, the gap between vanes in *N. hollandicus* rectrices persisted for a much longer portion of the feather germ and was an average of 0.5 ± 0.3 mm wide at the distal measure of new barb locus angle (Fig. 8d). The gap in *N. hollandicus* rectrices primarily closed by expanding the edge of the narrower, leading vane toward the relatively stationary edge of the trailing vane (Fig. 8d,e). Once the gap between vane edges closed in all feather types, the resulting single new barb locus maintained a relatively stable position throughout the rest of development (Fig. 8). The new barb locus in coverts was positioned at the ventral midline of the feather germ (Fig. 8a–c), and in rectrices it was displaced toward the leading edge of the rachis (Fig. 8d–g).

As feather development progressed, the rachis in both coverts and rectrices increased in width to take up a larger proportion of the feather germ. Even if there were no change in the position of the new barb loci, increases in the size of the rachis would result in a decrease of the new barb locus angle for each vane. This effect is the apparent reason for the slight proximal decreases in new barb locus angle of rectrix trailing vanes (Figs. 7g,h, Fig. 8d–g).

Finally, feather branches were highly compacted within the developing feather germ compared to after they had unfurled from the sheath at maturity. The width of mature feathers was on average 2–3 times greater than their width during development. Even though increasing feather germ diameter does contribute to a wider feather, this suggests that barb expansion plays a much more significant role in determining mature feather width. Barb expansion caused both rectrices and coverts to more than double in width as they unfurled from the relatively narrow circumference of the feather germ.

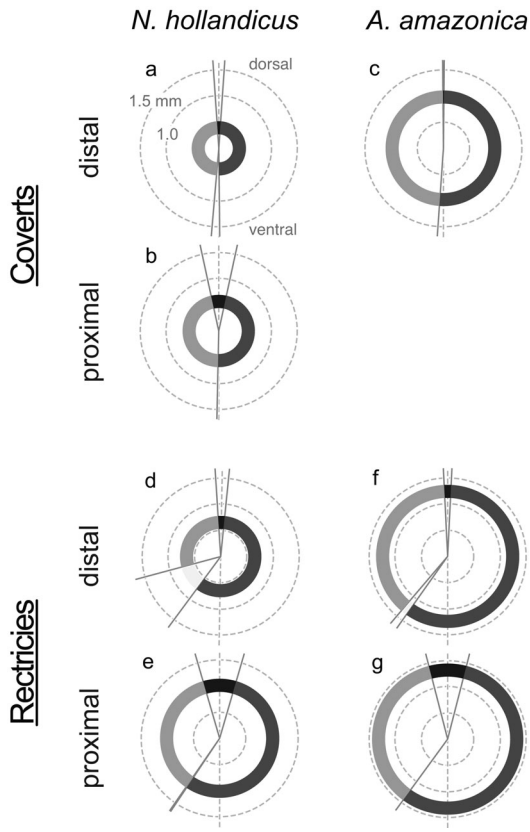

Figure 8. Cross-sectional views of developing feather germs showing the average radial positions of the rachis (black), trailing vane (dark gray), leading vane (gray), and gaps between feather vane edges (light gray). All feathers increase in diameter as development progresses proximally. Conversely, the positions of new barb loci (represented by the vane edge) remain relatively fixed throughout development with the exception of the leading vane of *N. hollandicus* rectrices (d–e). New barb loci are positioned roughly 180° opposite of the rachis in symmetrical covert feathers and offset toward the leading vane in asymmetrical rectrices.

DISCUSSION

Our theoretical models of vane width confirm that the morphological and developmental basis of vane asymmetry is both complex and redundant. Asymmetry in vane width could be driven by two independent morphological characters that are each in turn under the control of multiple developmental processes. As a result, there are many different possible combinations of

developmental modifications that could cause vane width asymmetry in a given feather. We obtained empirical measurements for all model parameters and were able to identify the combination of modifications responsible for vane asymmetry in real feathers. Both barb length and barb angle contributed to vane width asymmetry in rectrices as a result of dynamic changes in the trailing vane. Asymmetry in barb length was driven by a displacement of radial position of the new barb loci toward the leading edge of the rachis, and asymmetry in barb angle was driven by greater barb expansion in the trailing vane. The minor role of helical angle suggests that barb angle and barb length are essentially independent morphological characters that are each controlled by a different developmental process.

Helical Angle

Our results provide a good example of the utility of theoretical morphospace modeling. Our models describe the basic geometry of tubular feather development and the potential axes of variation, which include helical angle. However, we found that the changes in helical angle during development were always small, even in highly asymmetric feather, and in the wrong direction to positively contribute to vane width asymmetry. Though helical angle does not appear to contribute to vane width asymmetry in real feathers, this result raises the explicit question of why not? Nearly invariant helical angle could be indicative of a functional constraint, which gives a selective advantage to asymmetric feathers that do not vary in helical angle, or a developmental constraint, which gives little to no capacity to independently vary helical angle between the two vanes of a developing feather.

Barb Expansion

We found that barb expansion plays a profoundly important role in determining mature feather shape. Barb expansion was responsible for more than doubling the total width of feathers as they unfurled from the relatively narrow tubular feather germ. Moreover, expansion angle was the main contributor to mature barb angle for a given barb, as well as the main driver of barb angle variation, and subsequently vane width variation, within a feather. These results attest to the importance of this previously underappreciated developmental process.

The developmental and morphological control of barb expansion angle is not well understood. The ramus is complex multicellular structure with a solid beta-keratin cortex and an air-filled medullary pith that is attached to the rachis by a ribbon-like, solid keratin petiole (Lucas and Stettenheim, '72; Maderson et al., 2009). The intrinsic structure and complex material composition of these structures could play a role in driving barb expansion (Lingham-Soliar and Murugan, 2013). Alternatively, the dynamic interactions between barbules of neighboring barbs that form the coherent feather vane could physically constrain the extent of barb expansion (Prum and Williamson, 2001). Barb vanule width is dependent on barbule angle and length (Ennos et al., '95), suggesting that morphological changes in barbules could then affect the degree of barb expansion.

The presence of curved barbs in mature feathers indicates that either helical angle and or expansion angle must be dynamic along the length of developing barbs from tip to rachis. Based on our observations of feather germs, we suspect that little if any of the barb curvature occurs as a result of changes in helical angle. Instead, we predict that much of barb curvature is the result of *differential expansion along the length* of the barbs. Rami will certainly need to be flexible enough to facilitate barb curving during expansion, however, we hypothesize that the main driver to differential expansion is changes in vanule width. We have observed that the vanules of curved barbs taper strongly toward the barb tip, and this could force barb tips to curve in toward each other as they connect to form a coherent vane.

New Barb Locus

As previous researchers have predicted, we found that the relative position of the new barb locus, or loci, within the developing feather germ plays an important role in determining barb length and subsequently vane width asymmetry. Experimental perturbations of *Wnt* expression within a feather germ suggests that dorsal-ventral gradients of *Wnt* are at least in part responsible for the position of the new barb locus and for helical growth (Yue et al., 2006). These results were corroborated with a theoretical activator-inhibitor model that was able to simulate helical patterns with the addition of a third dorsal-ventrally polarized gradient (Harris et al., 2005). In combination, the theoretical and empirical results suggest that sonic hedgehog, *Bmp* and *Wnt* signaling cascades work in concert in a Turing-like, activator-inhibitor mechanism to pattern the barb ridges (Harris et al., 2002, 2005; Yue et al., 2006).

There have been no empirical or theoretical investigations on the molecular control of an offset new barb locus, gaps between vane edges, or the general arrangement of the feather tip. An offset new barb locus would imply an asymmetric *Wnt* gradient within the feather germ, whereas gaps between vane edges at the feather tip could potentially be due to a threshold effect that defines a boundary to barb ridge patterning within the larger feather germ. A better understanding of the control of asymmetric and discontinuous patterning within the feather germ would be of profound general interest.

Comparison With Previous Models

Prum and Williamson (2001) proposed the first integrated theoretical model of feather shape development. Our observations confirm a number of their predictions, including the effects of barb expansion on mature barb angle and subsequently vane width. However, our observations of developing feathers falsify a fundamental assumption of the Prum and Williamson (2001) model. Based on images of feather germs with a continuous ring of barb ridges, Prum and Williamson (2001) hypothesized that

both the position of the new barb locus, and the diameter of the feather germ were emergent properties of the barb ridges. In their model, feather germ diameter could only change as a direct result of changes in the number and size of barb ridges, and displacement of the new barb locus occurred only by the differential addition of new barb ridges to one side of the developing feather germ.

This view is not consistent with the observations that, in both embryonic feathers (Harris et al., 2002) and definitive feathers (Fig. 1d), barb ridges begin development on the dorsal midline, and new barb ridge addition advances independently on both sides of the feather germ toward the ventral side. During this early portion of development, barb ridges do not completely fill the feather germ (Fig. 1d) and new barb addition to one vane can proceed independently of the other vane. In light of these observations, we have modeled feather germ diameter and the relative position of the new barb locus for each vane as specified model parameters rather than as emergent properties of barb characters.

With our new model it is now possible to model a feather tip with separated vane edges within the feather germ even while the mechanisms responsible for specifying the new barb locus remains largely unknown. Second, the implied developmental causality of feather germ diameter in the model now more closely agrees with empirical descriptions of feather germ development. In the first generation of embryonic feathers the short bud has a diameter in the complete absence of barb ridges (Harris et al., 2002). In all successive feather generations, cell proliferation occurs at the base of the feather follicle and before differentiation of the feather germ into the various parts of the feather (Lucas and Stettenheim, '72; Yu et al., 2002). The diameter of the feather germ must therefore be determined well before the differentiation of any barbs, rather than as a direct result of barb characters as implied by the Prum and Williamson (2001) model.

Vane Folding. Alibardi (2009) proposed that in-folding of the vanes within the developing feather germ could be a mechanism for increasing feather width beyond the circumference of the feather germ, particularly in asymmetric feathers. However, we suspect that the vane folding within the feather germ reported by Alibardi (2009) may be an artifact from plucking or sectioning of the germs. Figures 4c and 5a of Alibardi (2009) show cross-sections of developing feather germs where the vane appears to have folded in, but other areas of the same cross-sections have apparently missing or distorted barb ridges.

We have found that plucking feather germs can cause a significant amount of damage to developing feather vanes, even while leaving the surrounding sheath undamaged (Fig. 1d). In almost all of the feather germs that we plucked, vanes were crumpled, separated, and folded back in on themselves for up to 5 mm both above and below where the feather germ was physically grasped for plucking. We found no evidence of vane folding beyond the portion of the feather germ immediately surrounding where the feather germ was grasped. In the absence of conclusive evidence of natural vane folding we did not include vane folding as a parameter in our model.

CONCLUSIONS

The development of an individual feather is a dynamic process both between vanes and across the length of a single feather germ. Our theoretical model revealed that many different possible combinations of developmental processes could be responsible for vane asymmetry in a given feather. We found that vane width asymmetry in parrot rectrices was driven by only two of the three potential developmental processes; displacement of the new barb ridge locus away from the ventral midline of feather germ followed by differential expansion of barbs as they unfurled from the sheath. Conversely, the helical angle of barb ridge development within the feather germ does not appear to play an appreciable role in vane width asymmetry, suggesting a possible functional or developmental constraint that prevents variation in this angle.

We provide the first empirical estimates of barb expansion angle and demonstrate its ability to vary within a feather. Estimates of expansion angle are unavailable for other species, but asymmetry in barb angle is a common character of flight feathers (Lucas and Stettenheim, '72; Ennos et al., '95). An offset new barb locus has been previously noted in domestic chicken (Hosker, '36), Zebra Finch (Alibardi, 2009), and homing Pigeon (Strong, '02). This suggests that differential barb expansion and an offset new barb locus in asymmetric feathers are common developmental modifications across extant birds (Hackett et al., 2008).

Prum ('99) proposed that the evolution of the asymmetric vane was among the most derived developmental innovations (Stage V) in the evolutionary diversification of feather morphology. Here, we have established that in addition to the radial displacement of the new barb locus, the lateral differentiation in barb expansion angle represents a second developmental innovation involved in the evolution of asymmetrical feather vanes. These two innovations are likely the result of fundamentally distinct developmental modifications; the former relying on changes in the molecular signals that pattern the feather during morphogenesis, and the latter relying on changes in cell size, composition and number. This speaks to both the complexity and hierarchy of processes involved in the evolution of asymmetric feathers.

ACKNOWLEDGMENTS

The authors would like to thank Gail Patricelli for hosting TJF at UC Davis and providing logistical support with IACUC protocols. Jacqueline Pisenti and Kristy Smith, managers of the UC Davis avian facilities, for help with all things bird related. Rebbeca Koch and Stacie Picone for assistance with feather plucking. This research benefited from input by Suzanne Alonzo, April

Dinwiddie, Todd Harvey, and Jacob Musser. Live animal work was approved under UC Davis IACUC protocol # 16650. Funding provided by the NSF graduate research fellowship program, Yale EEB Department Chair's Fund, and the Yale W. R. Coe Funds.

LITERATURE CITED

Alibardi L. 2009. Follicular patterns during feather morphogenesis in relation to the formation of asymmetric feathers, filoplumes and bristles. Ital J Zool 76:279–290.

Badyaev AV, Landeen EA. 2007. Developmental evolution of sexual ornamentation: model and a test of feather growth and pigmentation. Integr Comp Biol 47:221–233.

Bleiweiss R. 1987. Development and evolution of avian racket plumes: fine structure and serial homology of the wire. J Morphol 194: 23–39.

Brakefield PM. 2006. Evo-devo and constraints on selection. Trends Ecol Evol 21:362–368.

Brakefield PM. 2011. Evo-devo and accounting for Darwin's endless forms. Philos Trans R Soc B 366:2069–2075.

Campàs O, Mallarino R, Herrel A, Abzhanov A, Brenner MP. 2010. Scaling and shear transformations capture beak shape variation in Darwin's finches. Proc Natl Acad Sci USA 107:3356–3360.

Chandler AC. 1914. Modifications and adaptations to function in the feathers of *Circus hudsonius*. Univ Calif Publ Zool 11:329–376.

Ennos AR, Hickson JRE, Roberts A. 1995. Functional morphology of the vanes of the flight feathers of the pigeon *Columba livia*. J Exp Biol 198:1219–1219.

'Espinasse PG. 1939. The developmental anatomy of the Brown Leghorn breast feather, and its reactions to oesterone. Proc Zool Soc Lond 109:247–288.

Feduccia A, Tordoff HB. 1979. Feathers of Archaeopteryx: asymmetric vanes indicate aerodynamic function. Science 203:1021.

Hackett SJ, Kimball RT, Reddy S, et al. 2008. A phylogenomic study of birds reveals their evolutionary history. Science 320:1763–1768.

Hallgrímsson B, Jamniczky HA, Young NM, et al. 2012. The generation of variation and the developmental basis for evolutionary novelty. J Exp Zool (Mol Dev Evol) 318B:501–517.

Harris M, Fallon J, Prum RO. 2002. *Shh-Bmp2* signaling module and the evolutionary origin and diversification of feathers. J Exp Zool 294:160–176.

Harris M, Williamson S, Fallon J, Meinhardt H, Prum RO. 2005. Molecular evidence for an activator-inhibitor mechanism in development of embryonic feather branching. Proc Natil Acad Sci USA 102:11734–11739.

Hosker A. 1936. Studies on the epidermal structures of birds. Philos Trans R Soc Lond B Biol Sci 226:143–188.

Landeen E, Badyaev A. 2012. Developmental integration of feather growth and pigmentation and its implications for the evolution of diet-derived coloration. J Exp Zool Mol Dev Evol) 318B:59–70.

Lin CM, Jiang TX, Widelitz RB, Chuong CM. 2006. Molecular signaling in feather morphogenesis. Curr Opin Cell Biol 18:730–741.

Lin SJ, Wideliz RB, Yue Z, et al. 2013. Feather regeneration as a model for organogenesis. Dev Growth Differ 55:139–148.

Lingham-Soliar T, Murugan N. 2013. A new helical crossed-fibre structure of β-keratin in flight feathers and its biomechanical implications. PLoS ONE 8:e65849.

Longrich N, Vinther J, Meng Q, Quanguo L, Russell AP. 2012. Primitive Wing Feather Arrangement in *Archaeopteryx lithographica* and *Anchiornis huxleyi*. Curr Biol 22:2262–2267.

Lucas AM, Stettenheim PR. 1972. Avian anatomy—integument. Washington, DC: US Department of Agriculture Handbook.

Maderson PFA, Hillenius WJ, Hiller U, Dove CC. 2009. Towards a comprehensive model of feather regeneration. J Morphol 270:1166–1208.

McGhee GRJ. 1999. Theoretical morphology: the concepts and its applications. New York, NY: Columbia University Press.

Norberg R. 1985. Function of vane asymmetry and shaft curvature in bird flight feathers; inferences on flight ability of Archaeopteryx. In: Hecht MK, Ostrom JH, Viohl G, Wellnhofer P, editors. The beginnings of birds. Eichstätt, Germany: Freunde des Jura-Museums Eichstätt. p 303–318.

Palmer A. 2009. Animal asymmetry. Curr Biol 19:R473–R477.

Prum R. 1999. Development and evolutionary origin of feathers. J Exp Zool 285:291–306.

Prum RO, Williamson S. 2001. Theory of the growth and evolution of feather shape. J Exp Zool 291:30–57.

Prum R, Dufresne E, Quinn T, Waters K. 2009. Development of colour-producing β-keratin nanostructures in avian feather barbs. J Roy Soc Interface 6:S253–S265.

Speakman J, Thomson S. 1994. Flight capabilities of Archaeopteryx. Nature 370:514.

Strong RM. 1902. The development of color in the definitive feather. Bull Mus Comp Zool, Harvard College 40:147–185.

Xu X, Zhou Z, Wang X, et al. 2003. Four-winged dinosaurs from China. Nature 421:335–340.

Yu M, Wu P, Widelitz RB, Chuong C. 2002. The morphogenesis of feathers. Nature 420:308–312.

Yue Z, Jiang T, Widelitz RB, Chuong C. 2005. Mapping stem cell activities in the feather follicle. Nature 438:1026–1029.

Yue Z, Jiang T, Widelitz RB, Chuong C. 2006. Wnt3a gradient converts radial to bilateral feather symmetry via topological arrangement of epithelia. Proc Natl Acad Sci USA 103:951–955.